JOURNAL OF THERMOPHYSICS AND HEAT TRANSFER
Vol. 15, No. 4, October–December 2001

Analysis of a Single-Layer Thermophotovoltaic System at Moderate Temperatures

Linda Z. Shi,* Spencer Y. Xu,* and R. F. Boehm†
University of Nevada, Las Vegas, Las Vegas, Nevada 89154-4027

A study of a parallel-plate system for thermophotovoltaic power production at moderate temperatures is reported. The impetus behind this analysis is the desire to apply systems of this type in microdevices where large temperature differences would be difficult to sustain. The emphasis is on the combination of the photovoltaic (PV) modeling (which has been relatively well documented in the literature) with the thermal transport aspects, particularly the radiative properties, which have been addressed less fully. Of the latter, the monochromatic emissivity is defined in detail. $In_{0.8}Ga_{0.2}As$ is considered as the basic PV material, and two emitter surface treatments are assumed in the analysis including the gray approximation and both an idealistic and a realistic selective surface. Estimates of both the power generation and the power generation efficiency are determined. As expected for temperature differences of these magnitudes, the energy production is shown to be quite small.

Nomenclature

c_o = speed of light in a vacuum, 3.0×10^8 m/s
E = emissive power, W/m^2
Eg = bandgap energy, eV
e = electron charge, -1.602×10^{-19} C
h = Planck's constant, 6.626×10^{-34} J s
I_d = dark current, A/m^2
I_{sc} = open-circuit current, A/m^2
K_b = Boltzmann's constant, 1.381×10^{-23} J/K
k = extinction coefficient
n = index of refraction
P = electrical power generated, W/m^2
q = heat transfer, W/m^2
q_0 = radiosity, W/m^2
V_{oc} = open-circuit voltage, V
x = fraction Ga in $In_{x-1}Ga_xAs$
α = absorptivity
ε = emissivity
η = energy conversion efficiency (heat transfer to power)
η_{pv} = quantum efficiency of photovoltaic (PV) cell
λ = wavelength, μm
ν = quantity defined after Eq. (8)

Subscripts

b = blackbody
qn = quantum
λ = monochromatic
1 = emitter surface
2 = PV surface

Introduction

INTEREST has been developing in electrical and mechanical systems on the microscale. The literature is filled with reports of a variety of applications. One issue of interest in some of these systems is the conversion of thermal energy to electrical power. A possible method of doing this is with thermophotovoltaic (TPV) devices. In this approach, an emitter surface (higher temperature) opposes a photovoltaic (PV) surface (lower temperature). Radiation between the two surfaces generates electrical power. One of the problems associated with TPV systems at moderate temperatures is low-power conversion efficiency. However, on the microscale, high-temperature differences will be difficult to maintain across very small distances.

The TPV literature tends to focus on developments on either the PV cell side or the emitter side in the temperature range 1000–2500 K. Although conclusions from previous work are not directly related to thermal performance in the temperature range of interest in this study (360–560 K), it is helpful to consider aspects of this previous work.

Wojtczuk et al.[1] discussed $In_{1-x}Ga_xAs$ TPV cell performance vs bandgap. (There is some variation in the literature about how the fraction of the components is denoted, some authors using x for the fraction of In, whereas others use x for the fraction of Ga. We take the latter approach here.) The results showed that the 0.64-eV bandgap ($In_{0.62}Ga_{0.38}As$) cell had the highest power output for the range of temperatures they considered.

Models of low-bandgap solar cells for TPV applications were proposed by Jain et al.[2] The modeling results showed that $In_{0.53}Ga_{0.47}As$ cell (0.75-eV) efficiencies exceeding 30% were achievable for the Er–YAG selective emitter source at 1500 K when the cell's series resistance was reduced.

Wilt and Chubb[3] reported on TPV energy conversion technology development at the NASA John H. Glenn Research Center. They have applied selective emitters that demonstrated in-band emittances higher than 0.7 and out-of-band emittances lower than 0.2 at 1500 K.

Gray and El-Husseini[4] reported a parametric study of TPV system efficiency and output power density based on a simple endoreversible thermodynamic engine model of the TPV system. This study showed that the optimum TPV cell bandgap depended not only on the emitter spectrum, but also on the type and effectiveness of the spectral selection.

Adair and Rose[5] discussed using selective emitters to increase system efficiency. Good et al.[6] presented an optimization study of a selective emitter TPV system. They developed a computer model that incorporates detailed descriptions of the individual system components, such as representation of the selective emitter component based on the approximation of a rare-earth selective emitter.[7–9] The model predicted the component efficiencies, the overall system efficiency, and the system output power density for variations in the emitter temperature, the spectral emissivity and emission bandwidth of the emitter, the PV cell bandgap energy, the cell back-surface reflectivity, and the long-wavelength emission bandlimit of the emitter.

A recent study by Fatemi et al.[10] presented high-efficiency converters for TPV applications. These converters were built and tested

Received 11 December 2000; revision received 25 June 2001; accepted for publication 26 June 2001.

*Graduate Research Assistant, Mechanical Engineering.
†Director, Center for Energy Research, Box 454027, Howard R. Hughes College of Engineering.

at 1700 K. The test data showed that the Er–YAG selective emitter with 0.69-eV PV cell converter has the highest energy efficiency (approaching 30%), and the wideband emitter (with bandpass/infrared reflector filter) with 0.69-eV PV cell converter has the highest electrical output power density near 2 W/cm^2.

There exists a common point in all of the mentioned studies. The temperature range of the emitter side is from 1000 to 2500 K. Most applications strive for high electrical power output, and therefore, high temperatures are needed.

On the other hand, there could be applications, for example, microdevices, where high-temperature differences cannot be tolerated. What will happen if the temperatures on the emitter side are in the range 360–560 K? What electrical output power densities can be generated with the same converter, used in the temperature range 1000–2500 K? It is obvious at the outset that these performance parameters will decrease. However, several variations may be possible in microscale that are not feasible in the more commonly investigated systems noted earlier. These include layering of systems and use of very small (on the order of the size of the wavelength) spacings.[11,12] Attention will be given to these aspects in later papers.

From a microscale point of view, a flat plate system is easily manufactured and assembled for both the PV cell side and the emitter side. The thermal analysis presented here is based on an evacuated flat parallel-plate geometry.

Description of the Model

Basic Equations

The thermal behavior of an evacuated flat parallel-plate system consisting of a selective emitter and a PV material is analyzed in the present study. The separation spacing is assumed to be large compared to the wavelength of the radiation but small compared with the size of the parallel plate. Edge effects are neglected.

The model used is based on traditional formulations for the radiative exchange. The spectral, blackbody emissive power is given by[13]

$$E_{\lambda,b} = \frac{2\pi h c_0^2}{\lambda^5[\exp(hc_0/\lambda K_b T) - 1]} \tag{1}$$

This is then used to find the spectral net heat transfer between two surfaces,[13]

$$q_\lambda = \frac{E_{\lambda,b1} - E_{\lambda,b2}}{(1/\varepsilon_{\lambda 1} + 1/\varepsilon_{\lambda 2} - 1)} \tag{2}$$

The irradiation on the PV material is needed to determine its power output. For an infinite parallel-plate system, this is the same as the radiosity from the selective emitter surface,[13]

$$q_{\lambda,o1} = E_{\lambda,b1} - [(1 - \varepsilon_{\lambda 1})/\varepsilon_{\lambda 1}]q_\lambda \tag{3}$$

With this and the quantum efficiency, the short-circuit current of the PV material can be found:

$$I_{sc} = \frac{e}{hc_o}\int_{\lambda_i}^{\lambda_f} \lambda \eta_{\mathrm{pv}\lambda} q_{\lambda,o1}\, \mathrm{d}\lambda \tag{4}$$

Note that this equation gives some cause for concern. It is based on the conventional definition of quantum efficiency used in a variety of devices (for example, see Refs. 14 and 15), where the power output is determined from the incident intensity (the radiosity of the opposite surface for the geometry considered here). For higher-temperature systems, the usual case considered in TPV configurations, this does not cause a problem. For the lower temperature arrangements here, there is still a radiosity even at zero temperature difference, which can yield a short-circuit current in this limit. This could lead to an apparent violation of energy conservation.

The dark saturation current can then be determined.[16] At 300 K, the following holds:

$$I_d = 1.5 \times 10^9 \exp(-Eg/K_b T) \tag{5}$$

and the bandgap can be represented by[11]

$$Eg = 0.35 + 0.5x + 0.59x^2 \tag{6}$$

where x is the fraction of Ga in $In_{1-x}Ga_xAs$ (see more discussion of this subsequently). As given by Green,[16] the open-circuit voltage is determined from

$$V_{\mathrm{oc}} = (K_b T/e)\, \ell n(I_{sc}/I_d + 1) \tag{7}$$

whereas the fill factor (FF) is given by

$$\mathrm{FF} = [v - \ell n(v + 0.72)]/(v + 1) \tag{8}$$

where

$$v \equiv V_{\mathrm{oc}}/K_b T/e$$

Sufficient parameters have been found at this point that the power output can be determined

$$P = I_{sc} V_{\mathrm{oc}} \mathrm{FF} \tag{9}$$

The monochromatic heat transfer across the gap given in Eq. (2) is used to find the total heat transfer by integrating over all wavelengths. At this point, the efficiency can be found:

$$\eta = P/q \tag{10}$$

In this equation, the total heat transfer is used:

$$q = \int_0^\infty q_\lambda\, \mathrm{d}\lambda \tag{11}$$

The PV material is assumed to be held at 300 K in all cases. The emitter surface was taken in a range of higher temperatures between 360 and 560 K.

PV Materials Considered

Long-wavelength PV materials are usually the alloys from the III–V and IV families of semiconductors such as compounds of InGaAs, InSb, GaSb, GaInSb, SiGe, InAs, InAsP, InAlAs, GaAsSb, and Ge. These materials fall in the bandgap range between 1.1 and 0.36 eV. This range of bandgaps offers many choices for the various wideband and narrowband emission sources for TPV applications.[2] High efficiency PV cells can be made of indium gallium arsenide ($In_{1-x}Ga_xAs$), and the Ga composition x can be varied to change the bandgap range from GaAs ($x = 1.0$, 1.42 eV, 0.9-μm cutoff wavelength) to InAs ($x = 0$, 0.36 eV, 3.4-μm cutoff wavelength). This allows the PV cell bandgap to be spectrally matched to the heat source to maximize electrical power output.[1] Compounds of $In_{1-x}Ga_xAs$ have become popular for PV converters.[17]

In this study we focus on $In_{0.8}Ga_{0.2}As$ (bandgap energy = 0.48eV) throughout. Preliminary investigations indicated that the other typical formulations yielded lower values of power output and efficiency for the temperature range of interest.

Spectral Emissivity of the PV Material

It is difficult to find tabulated emissivities for $In_{0.8}Ga_{0.2}As$. In this study, emissivities were estimated from optical constant tabulations.

First, the spectral data for index of refraction and extinction coefficient for $In_{0.8}Ga_{0.2}As$ were selected.[11] These are shown in Fig. 1.

With the n and k given, the monochromatic hemispherical emissivity can be found. A closed-form expression for this is given by Siegel and Howell[13]:

$$\begin{aligned}\varepsilon_\lambda = {} & 4n_\lambda - 4n_\lambda^2\, \ell n \frac{1 + 2n_\lambda + n_\lambda^2 + k_\lambda^2}{n_\lambda^2 + k_\lambda^2} \\ & + \frac{4n_\lambda\left(n_\lambda^2 - k_\lambda^2\right)}{k_\lambda} \tan^{-1}\left(\frac{k_\lambda}{n_\lambda^2 + k_\lambda^2}\right) \\ & + \frac{4n_\lambda}{n_\lambda^2 + k_\lambda^2} - \frac{4n_\lambda^2}{\left(n_\lambda^2 + k_\lambda^2\right)^2}\, \ell n\left(1 + 2n_\lambda + n_\lambda^2 + k_\lambda^2\right) \\ & - \frac{4n_\lambda\left(-n_\lambda^2 + k_\lambda^2\right)}{k_\lambda\left(n_\lambda^2 + k_\lambda^2\right)^2} \tan^{-1}\frac{k_\lambda}{1 + n_\lambda}\end{aligned} \tag{12}$$

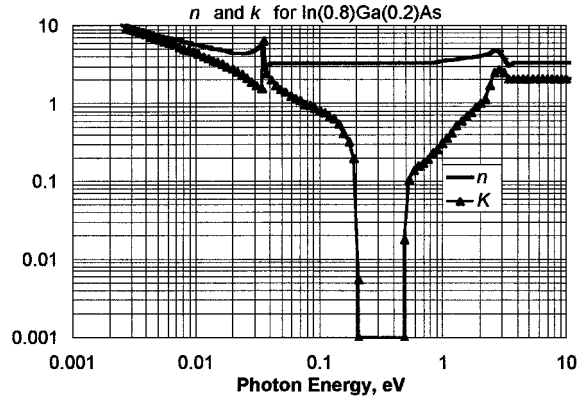

Fig. 1 Refractive index n and extinction coefficient k of $In_{0.8}Ga_{0.2}As$ as a function of wavelength (adapted from Whale[11]).

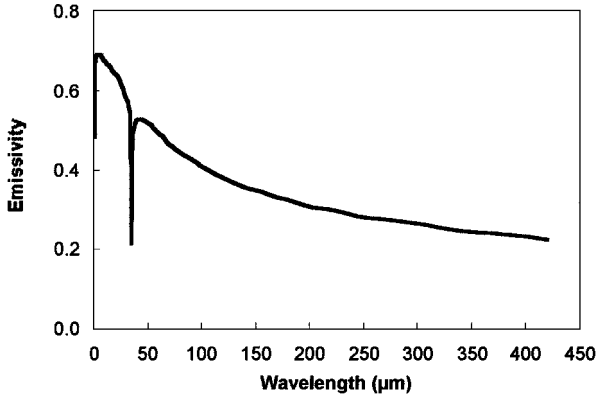

Fig. 2 Emissivity of $In_{0.8}Ga_{0.2}As$ over broad wavelength range.

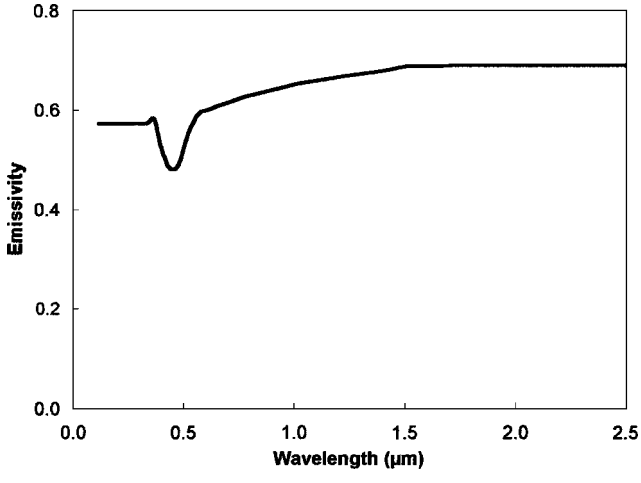

Fig. 3 Details in the wavelength range of PV interest of the emissivity variation of $In_{0.8}Ga_{0.2}As$; compare to Fig. 2.

This equation is developed from electromagnetic theory and is for monochromatic values. An approximation in the development of this result is that $\sin^2\theta$ (where θ is the angle of incidence of the incoming rays) can be neglected compared to $n_\lambda^2 + k_\lambda^2$. A check of this latter sum showed that the requirement was met virtually throughout the whole wavelength range. Comparisons were made to the method of Hering and Smith,[18] and quite reasonable agreement was found. The resulting monochromatic variation of emissivity is shown in Fig. 2 for a wide range of wavelengths. Of great importance is the variation in the range where the quantum efficiency (shown in the next section) is nonzero because this range is used to determine the power output. Details of the emissivity in this range are shown in Fig. 3.

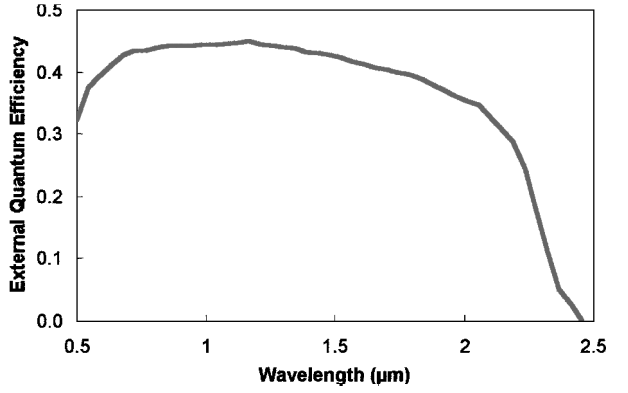

Fig. 4 Spectral variation of external quantum efficiency of $In_{0.8}Ga_{0.2}As$ (Ref. 17).

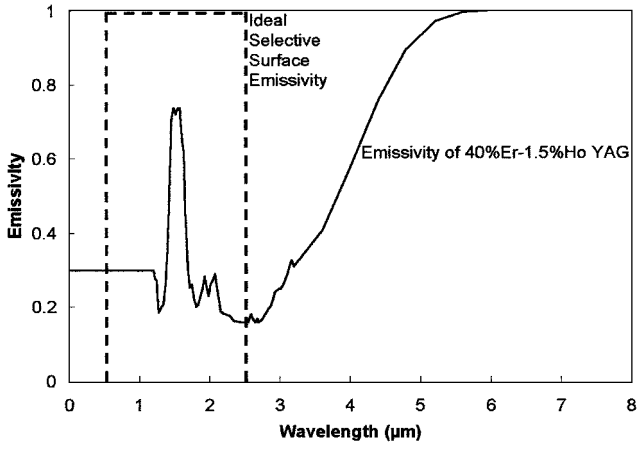

Fig. 5 Monochromatic emissivity of 40% Er–1.5% Ho YAG contrasted to an ideal selective surface; both lower (below 1.2 μm) and upper asymptote (above 3.2 μm) variations for the ErHo YAG are assumed because of lack of specific information. Intermediate wavelength values are from Ref. 9.

External Quantum Efficiency

The PV material's external quantum efficiency is defined as the ratio of the photogenerated carriers to the photon flux incident on the PV material. An antireflecting coating on the PV material can have a major influence on the external quantum efficiency. Here, only the external quantum efficiency of the PV material without an antireflecting coating was considered. Coutts et al.[17] present data for bandgaps of the $In_{1-x}Ga_xAs$ material of 0.49, 0.54, and 0.61 eV. We have used the values for 0.49 eV that actually represent the material $In_{0.79}Ga_{0.21}As$. Although there are differences between this and the material we have assumed, those differences will be small enough to be ignored here. These data are shown in Fig. 4.

Emissivity of Emitter

Three models for the emitter surface were assumed. These are described as follows:

1) For the gray surface portion of the study, the emissivity is taken to be invariant with wavelength, and the values were taken to vary from 0.1 to 1.0.

2) For the ideal selective surface model, the emitter surface is assumed to have an emissivity of value unity only in the wavelength range where the PV surface's quantum efficiency is nonzero. Elsewhere the emissivity is assumed as zero. This is shown in Fig. 5.

3) The third model is a representation of a real selective emitter. The rare-earth elements have a unique electronic structure that results in materials containing these elements emitting in a narrow band when heated.[5,19] In this work this is assumed to be a 40% Er–1.5% Ho YAG (yttrium aluminum garnet, $Y_3Al_5O_{12}$) thin-film selective emitter. The surface emissivity was estimated from data

given by Lowe et al.[9] for the wavelength range $1.2 < \lambda < 3.2$ μm, shown in Fig. 5. Note that values in the long-wavelength limit ($\lambda > 3.2$ μm) are not specified by Lowe et al. However, this wavelength range is important in the current work. We assume the variation to increase to unity in the range 3.2–6 μm and to stay at unity at longer wavelengths.[6,20]

Numerical Evaluation

MATLAB® 5.3 was used for the numerical simulation of the equations described earlier. In this software, the function for integration is QUAD. This involves an adaptive recursive Simpson's rule routine with a specified relative error.

Results and Discussion

The effect of the value of a gray emitter surface emissivity on TPV system power output is shown in Fig. 6. Note that the power output is not directly proportional to the emissivity of the emitter surface. The reason for this is that the emitter radiosity, which is used in the power output calculation, is heavily influenced by the PV radiosity in these low-temperature systems.

Figure 7 shows the power output for a system using a selective emitter. Here results for an ideal selective emitter are shown as the upper line. This ideal emitter is one where the monochromatic emissivity is unity in the range of nonzero quantum efficiency (see Fig. 4) and zero elsewhere. A more realistic output is shown for a ErHo YAG coated selective emitter surface (the lower curve). The power output for the ideal selective emitter matches that of a blackbody emitter, as shown in Fig. 6. On the other hand, the ErHo

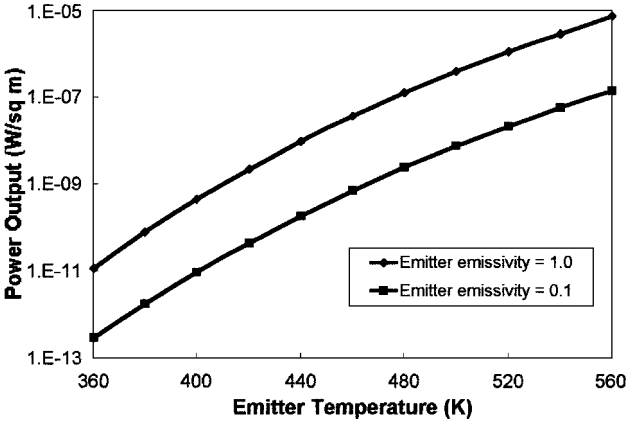

Fig. 6 Effect of gray emitter emissivity on power output from uncoated $In_{0.8}Ga_{0.2}As$ material at 300 K.

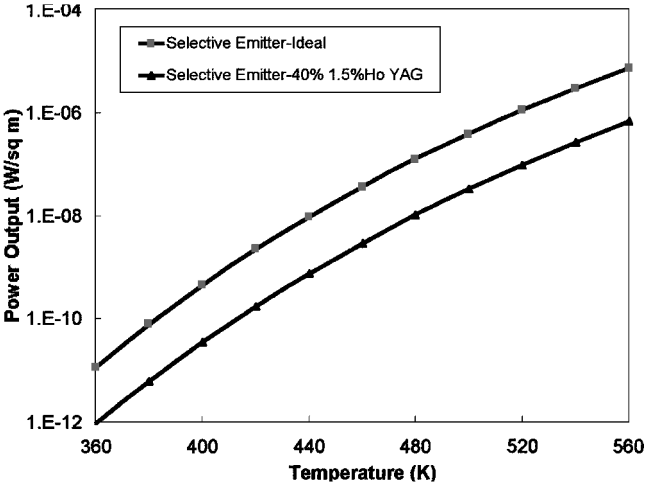

Fig. 7 Power output of TPV system consisting of uncoated $In_{0.8}Ga_{0.2}As$ material at 300 K with a 40%Er–1.5%Ho YAG emitter and an ideal selective emitter at various temperatures.

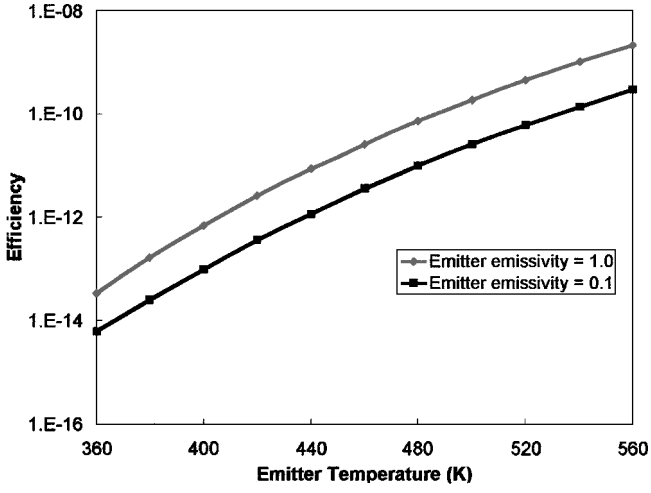

Fig. 8 System efficiency for various temperatures for $In_{0.8}Ga_{0.2}As$ PV material with a gray emitter; PV material held at 300 K.

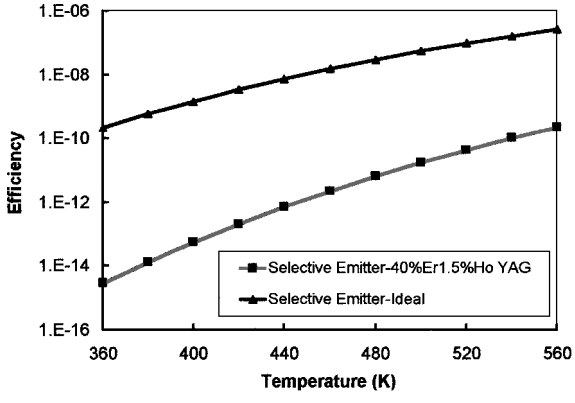

Fig. 9 System efficiency for the $In_{0.8}Ga_{0.2}As$ PV material contrasted for a selective emitter with a ErHo YAG coating (lower curve) and an ideal selective surface (upper curve); PV material held at 300 K.

YAG coated selective emitter surface curve falls between the two gray value variations shown in Fig. 6, as would be expected.

When the efficiency for the gray-emitter system is determined, the results vary as shown in Fig. 8. Normalizing the power output by the heat transfer in this manner represents nearly the same variation as before, with the ratios of the efficiency curves being less than that of the power output curves. The efficiency values are quite low due to the large amount of emission in the wavelength regions where the quantum efficiency is zero.

Now consider the variation of the system efficiency for the selective emitter cases. Results for these are shown in Fig. 9. For the ErHo YAG surface, small differences are seen between this one and the smaller-emissivity-valuecurve shown in Fig. 8. Also note the much higher value of efficiency shown for the ideal selective surface. This is due to both the very high emissivity in the active quantum efficiency range as well as the zero values outside of this range. As can be seen from Fig. 5, there is a great deal of difference between the two cases. It seems reasonable that a selective emitter will greatly increase system efficiency but will not effect the actual power generation to any extent compared to the black surface results.

The largest source of numerical errors in the results given arises primarily in the estimation of the monochromatic emissivities of the selective surface. Tabulated data for these properties are limited in the literature cited. Hence, estimated errors in the results determined with these approximations might be as high as 20%. However, the extent of the errors would not change the general trends shown.

As would be expected, the role of the PV surface (the lower-temperature surface) in the energy exchange is quite important in

these moderate temperature studies, and overall output is quite low. This is not the case to the same extent in the higher-temperature studies normally considered in the TPV work. However, as pointed out earlier, the microsystem applications offer the opportunity to use several physical features not typically available in more-common systems including stacking to cascade the effects and close spacings to take advantage of wave interference. These will be reported in later papers.

Summary

1) A study has been performed of a parallel-plate TPV system at moderate temperatures: the emitter temperatures in the range of 360–560 K, with the PV material temperature assumed to be 300 K throughout. The moderate temperatures are of interest for possible application in micromachines. Large (compared to the wavelength of the radiation) spacings between the surfaces are assumed, but edge effects are ignored.

2) $In_{0.8}Ga_{0.2}As$ is taken for the PV material throughout because this showed better performance compared to other typical compositions of this family of materials in preliminary calculations. Monochromatic values of hemispherical emissivity were calculated from optical constant data tabulated in the literature with the aid of electromagnetic wave theory.

3) Two different types of emitter surfaces were compared. One was a gray surface with emissivity treated parametrically over the range 0.1–1.0, and the other was a selective surface in one case consisting of ideal selectivity and the other utilizing a more realistic ErHo YAG coating.

4) It is clear that the power output is set by the quantum efficiency variation of the PV material and the emissivity variation of the emitter surface within that quantum efficiency wavelength range, as well as the two surface temperatures.

5) The system efficiency is greatly influenced by the net heat transfer, as well as the power generated, giving higher efficiency estimates for lower net heat transfer cases as would result from the use of selective surfaces.

6) Both power output and system efficiency are shown to be quite low. This may render the approach impractical for some applications. However, effects not included here, including the enhanced radiative transfer for surfaces very close to one another, could change this situation considerably.

7) Possible errors in the results are due to the assumed variations of the monochromatic quantum efficiency and monochromatic emissivity of the selective surface. These potential errors do not change the general trends shown.

References

[1]Wojtczuk, S., Gagnon, E., Geoffroy, L., and Parodos, T., "$In_{(x)}Ga_{(1-x)}As$ Thermophotovoltaic Cell Performance vs. Bandgap," *First NREL Conference on Thermophotovoltaic Generation of Electricity*, American Institute of Physics Press, Woodbury, NY, 1994, pp. 177–187.

[2]Jain, R. K., Wilt, D. M., Landis, G. A., Jain, R., Weinberg, I., and Flood, D. J., "Modeling of Low-Bandgap Solar Cells for Thermophotovoltaic Applications," *First NREL Conference on Thermophotovoltaic Generation of Electricity*, American Institute of Physics Press, Woodbury, NY, 1994, pp. 202–209.

[3]Wilt, D. M., and Chubb, D. L., "Thermophotovoltaic Energy Conversion Technology Development at NASA Lewis Research Center," *Proceedings of the ASME Advanced Energy Systems Division*, AES-Vol. 37, American Society of Mechanical Engineers, Fairfield, NJ, 1997, pp. 47–52.

[4]Gray, J. L., and El-Husseini, A., "A Simple Parametric Study of TPV System Efficiency and Output Power Density Including a Comparison of Several TPV Materials," *Second NREL Conference on Thermophotovoltaic Generation of Electricity*, American Institute of Physics Press, Woodbury, NY, 1995, pp. 3–15.

[5]Adair, P. L., and Rose, M. F., "Increased Thermophotovoltaic System Efficiency Using Selective Emitters," *Proceedings of the 30th Intersociety Energy Conversion Engineering Conference*, Vol. 1, ASME, New York, 1995, pp. 503–508.

[6]Good, B. S., Chubb, D. L., and Lowe, R. A., "Optimization Study of Selective Emitter Thermophotovoltaic Systems," *Proceedings of the 31st Intersociety Energy Conversion Engineering Conference*, Inst. of Electrical and Electronics Engineers, New York, Vol. 2, 1996, pp. 1007–1012.

[7]Adair, P. L., and Rose, F., "Composite Emitters for TPV Systems," *First NREL Conference on Thermophotovoltaic Generation of Electricity*, American Institute of Physics Press, Woodbury, NY, 1994, pp. 245–262.

[8]Nelson, R. E., "Grid-Independent Residential Power Systems," *Second NREL Conference on Thermophotovoltaic Generation of Electricity*, American Institute of Physics Press, Woodbury, NY, 1995, pp. 221–237.

[9]Lowe, R. A., Chubb, D. L., and Good, B. S., "Radiative Performance of Rare Earth Garnet Thin Film Selective Emitters," *First NREL Conference on Thermophotovoltaic Generation of Electricity*, American Institute of Physics Press, Woodbury, NY, 1994, pp. 291–297.

[10]Fatemi, N. S., Hoffman, R. W., Jr., Lowe, R. A., Jenkins, P. P., Garverick, L. M., Wilt, D. M., and Scheiman, D., "High Efficiency Converters for Thermophotovoltaic Applications," *Proceedings of the 31st Intersociety Energy Conversion Engineering Conference*, Vol. 4, Inst. of Electrical and Electronics Engineers, New York, 1996, pp. 2238–2242.

[11]Whale, M. D., "A Fluctuational Electrodynamic Analysis of Microscale Radiative Transfer and the Design of Microscale Thermophotovoltaic Devices," Ph.D. Dissertation, Dept. of Mechanical Engineering, Massachusetts Inst. of Technology, Cambridge, MA, June 1997.

[12]Pan, J. L., Choy, H. K. H., and Fonstad, C. G., "Very Large Radiative Transfer over Small Distances from a Black Body for Thermophotovoltaic Applications," *IEEE Transactions on Electron Devices*, Vol. 47, No. 1, 2000, pp. 241–249.

[13]Seigel, R., and Howell, J., *Thermal Radiation Heat Transfer*, 3rd ed., Hemisphere, New York, 1992, pp. 22, 121, 334.

[14]Corrons, A., and Zalewski, E., "Detector Spectral Response from 350 to 1200 nm Using a Monochromator Based Spectral Comparator," National Bureau of Standards, Washington, DC, TN 988, 1978, p. 4.

[15]Donati, S., *Photodetectors, Devices, Circuits, and Applications*, Prentice–Hall, Upper Saddle River, NJ, 2000, p. 9.

[16]Green, M. A., *Solar Cells: Operating Principles, Technology, and System Applications*, Prentice–Hall, Englewood Cliffs, NJ, 1982, Chaps. 4, 5.

[17]Coutts, T. J., Wanlass, M. W., Ward, J. S., and Johnson, S., "A Review of Recent Advances in Thermophotovoltaics," *Conference Record of the 25th IEEE Photovoltaics Specialists Conference*, Inst. of Electrical and Electronic Engineers, New York, 1996, pp. 25–30.

[18]Hering, R. G., and Smith, T. F., "Surface Radiation Properties from Electromagnetic Theory," *International Journal of Heat and Mass Transfer*, Vol. 11, 1968, pp. 1567–1571.

[19]Guazzoni, G. E., "High Temperature Spectral Emittance of Oxides of Erbium, Samarium, Neodymium and Ytterbium," *Applied Spectroscopy*, Vol. 26, No. 1, 1972, pp. 60–65.

[20]Chubb, D. L., Pal, A. T., Patton, M. O., and Jenkins, P. P., "Rare Earth Doped High Temperature Ceramic Selective Emitters," *Journal of the European Ceramic Society*, Vol. 19, 1999, pp. 2551–2562.